Developments of In Situ Microfluidic Radiochemical Systems for Pure β Emitting Radionuclides - 24301

Sarah E. Lu [a], Andrew Morris[b], Geraldine Clinton Bailey [b], Medya Namiq[c], Frances Burrell[a], Richard M. Marsh[a], Jake Ludgate[b], Christopher Cardwell[b], Reuben Forrester[b], Pawel Gaca[a] , Matthew C. Mowlem[b], Phillip E. Warwick[a]

a University of Southampton, UK
b National Oceanography Centre, Southampton, UK

ABSTRACT

In situ microfluidic radiochemical analysis holds significant potential as a disruptive monitoring technology within the nuclear industry, providing a viable alternative to conventional manual sampling methodologies. The results of our work demonstrate the capability to reduce material consumption and the requirement for specialist facilities for handling radioactive materials during the initial characterisation process. This constitutes the first step toward robust *in situ* microfluidic detection for pure β-emitting radionuclides capable of field deployment and integration with autonomous platforms to enable remote detection and monitoring to support radiochemical analysis. The results from prototype validation demonstrate its proficiency in detecting β particles via Cherenkov radiation, achieving a minimum detectable activity of 0.8 kBq and maximum clearance time of 22 minutes after a 50 kBq sample. Coupling of numerical modelling and radiometric validation established a $R^2 > 0.91$, demonstrating this approach as a potential method of rapid prototyping to inform and drive design enhancements.

INTRODUCTION

The development of *in situ* technologies for detecting pure β-emitting radionuclides has significant implications for the nuclear industry, enabling autonomous, real-time data collection in nuclear facilities. Lab-on-a-Chip (LoC) systems offer a streamlined solution, minimising waste production and manual sampling challenges. However, further research is needed to optimise LoC device integration with detectors [1]. While existing research has explored various applications, there is a notable gap in integrating optical detection methods [2,3] and developing technology for autonomy for continuous monitoring applications.

Numerical modelling plays a crucial role in optimising photon detection efficiency, particularly in radiometric LoC systems with small sample volumes. This approach offers a cost-effective alternative to immediate prototyping and has been previously successfully validated with experimental data with a non-radiological source of light [1]. To advance this technology, a prototype Microfluidic Detection Unit (MDU) was designed, fabricated, and integrated with a photomultiplier tube (PMT).

Results demonstrated that the prototype could detect β particles through the Cherenkov radiation under laboratory conditions with an average limit of detection of 23 counts with count times of 5 minutes over 12 hours with readings obtained every 30 minutes. The minimum detectable activity for the MDU prototype was 0.8 kBq. This study presents a novel approach utilising numerical modelling to address the gap in sustainable design for radiometric LoC systems. The results obtained from this research emphasise the importance of further validation and refinement for complex microfluidic systems for radiometric detection.

By advancing the field of LoC technology in the nuclear industry, this research has the potential to improve process control, reduced costs, and minimised environmental impact.

OPTICAL DETECTION: TARGET RADIONUCLIDE AND METHOD

The pure β emitter ^{90}Sr, a radionuclide known for its high fission from uranium-235, remains a key radionuclide of interest to the nuclear industry, particularly in the sectors of waste management and decommissioning [4].Given its industrial and environmental significance to the nuclear industry, ^{90}Sr was chosen as the target radionuclide for the development and testing of the experimental and modelled prototype system. β particles from ^{90}Sr will be emitted with a maximum energy of 546 keV, whilst β particles emitted from its daughter nuclei ^{90}Y will have a maximum energy of 2282 keV. The short half-life of ^{90}Y means that it is in secular equilibrium with ^{90}Sr prior to decaying to stable ^{90}Zr. These factors mean the capability for this radionuclide to emit a significant abundance of high-energy β particles compared to other pure β emitting radionuclides of interest (e.g., ^{3}H,^{99}Tc) makes it ideal for testing and development of a prototype.

The average kinetic energy (E_{avg}) of a β particle emitted from ^{90}Sr is ~ 182 keV which is below the Cherenkov threshold energy of 264 keV in water, whilst the E_{avg} of a β particle emitted from ^{90}Y is ~760 keV. Therefore, most Cherenkov photons produced will be from a ^{90}Y β particle emission, and a small proportion arising from β particles emitted from ^{90}Sr are above the Cherenkov threshold for water. The number of photons (*N)* emitted for a single β particle produced within the sample volume was estimated with the Frank-Tamm equation:

$$N = 2\pi\alpha x\left({}^{1}/_{\lambda_2} - {}^{1}/_{\lambda_1}\right)(\sin^2\theta_c) \qquad \text{(Eq.1)}$$

where α is the fine structure constant, x is the particle path length, λ_1 and λ_2 are the upper and lower limits of the selected wavelength region, respectively, and θ_c is the Cherenkov emission angle dependent on the emitted β particle energy.. The spectral region was defined as $3.0x10^{-5}$ and $8.5x10^{-5}$ cm. For ^{90}Y emitting a single β particle of E_{avg} with a maximum possible path length (x) of 0.28 cm in water, 81 photons are produced (without deceleration of the β particle).

The activity in the prototype was determined by calculating the maximum volume and activity of the solution in the prototype. It was estimated that 1/3 of the disintegration events resulted in the production of Cherenkov photons during a five-minute count time, and a detection efficiency of 0.1 was applied. Furthermore, it was assumed that the number of Cherenkov photons generated in the PMMA surrounding the channel were negligible.

PROTOTYPE PRODUCTION AND ASSEMBLY

The prototype microfluidic detection unit was designed using CAD software (Autodesk, Fusion 360) and was micro-milled (Datron Neo CNC, DATRON Dynamics, Inc, USA). After the prototype channels were milled they were solvent polished to obtain high-quality optical surfaces [5]. The prototype (Figure 1) consisted of channels made from PMMA (theplasticshop, UK).

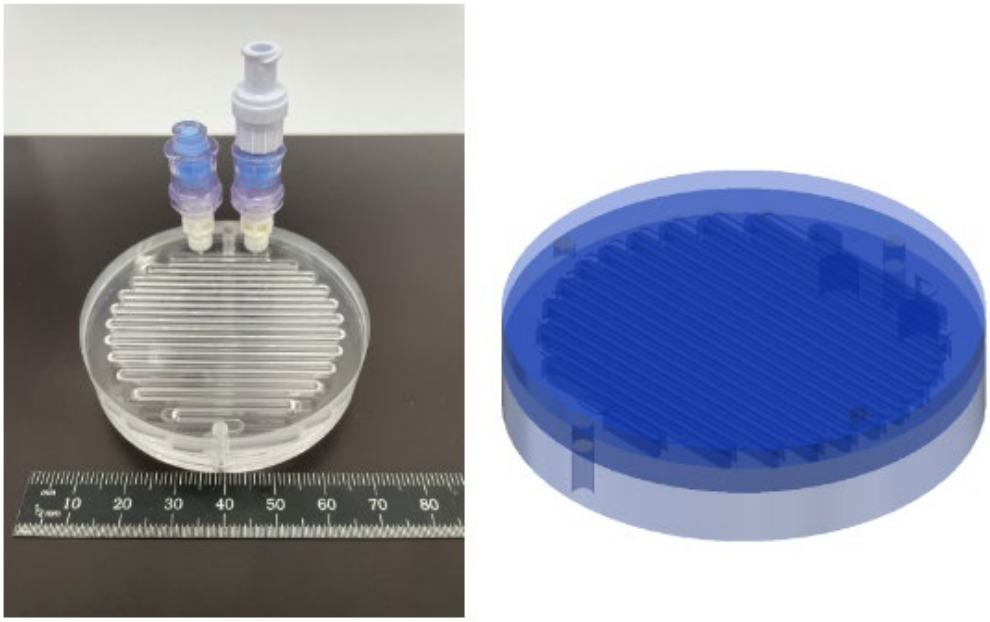

Figure 1. Picture and CAD Render (Autodesk, Fusion 360) of prototype.

The channel design (Figure 2) consisted of superimposed channels; the serpentine channel closest to the detector had a channel width of 0.8 mm wide and a depth of 0.5 mm, the superimposed channel was 0.8 mm wide and 3 mm deep to reduce the distance between photon production and the detector. For the second design both channels were filled sequentially from the same port. Adding a mirror behind the transparent test chips also assessed the impact of adding a reflective channel coating.

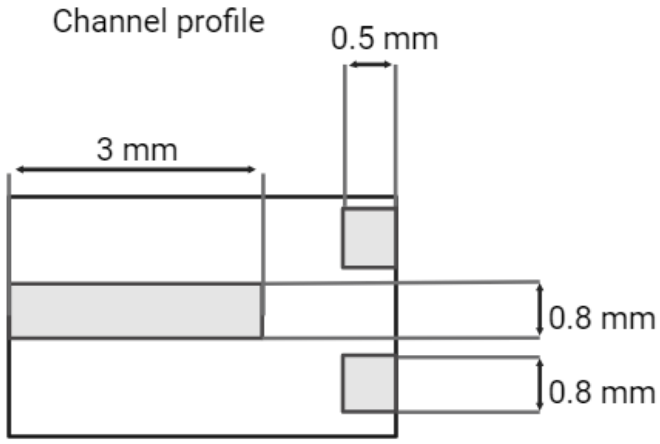

Figure 2. Diagram of channel profiles in prototype.

Microchannel geometry was micrographed (Zeta-20 Profilometer, KLA, USA) before experimentation to confirm channel dimensions and check for potential milling defects or blockages. The prototype was checked for leaks by flushing through coloured dye. At all times before reagents were introduced in the manifold, the prototype and tubing were cleaned by pumping UHP water (20 mins) followed by 0.1 M HCl (up to 10 mins) and then again flushed with UHP water (up to 20 mins). During the cleaning process the cell is then flushed with 10 mL of air to remove excess UHP water.

EXPERIMENTAL METHOD

A static system was developed to fill the prototype with ^{90}Sr/Y tracer. The ^{90}Sr/Y solution was loaded into the prototypes using disposable plastic syringes via a one-way valve. The prototype was fitted with two luer locks and a one-way valve system to prevent back flow from the contents of the prototype when loading or cleaning. The outlet was connected to an opening connector and a syringe with the plunger remove to allow fluid flow when loading and unloading the chip. To load the prototype a 5 mL syringe was connected to the one-way valve once outlet valve has been opened. When disconnecting the prototype, the syringe containing fluid/ or radionuclides was disconnected first.

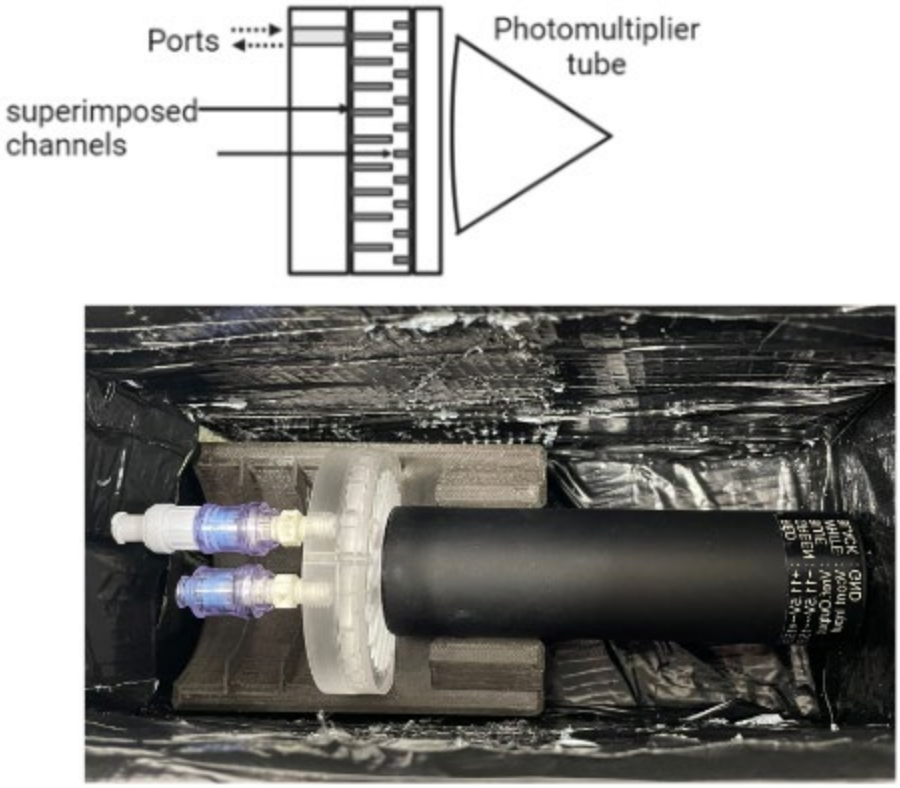

Figure 3. Picture of experimental setup for the radiological experiment and diagram orientation of prototype, setup is pictured without the blackout lid and sheets.

LINEARITY OF SYSTEM

The prototype was filled with six different activities of $^{90}Sr/^{90}Y$ ranging from 2.8 kBq to 13.6 kBq. Counts were recorded at 5-minute intervals to capture the system's response to changing activity levels, count measurements were recorded every 30 minutes for a minimum of 3 hours. The resulting plot of photomultiplier tube (PMT) output represents the counts accumulated during the 5-minute timeframe, corrected to account for background readings. The counts are then plotted against the corresponding activity (kBq) levels in the prototype (Figure 4). Prior to conducting the measurements, background readings were obtained for a duration of 3 hours to establish a baseline. The error bars in the plot represent the combined standard deviations of the background readings and repeated active count rates over the course of 3 hours. These readings were taken every 30 minutes to ensure accurate assessment. The results were obtained for both the opaque and reflective cases for the prototype. The objective of this approach was to evaluate the system's ability to detect and measure linear changes in activity levels. The results indicated that the system exhibited a linear response to changes in activity with potential slight after 12 kBq. This observation suggests that there may be potential quenching mechanisms in the system above 12 kBq. However, more experiments > 15 kBq are required to examine this further as linearity studies in radiometric LoC devices for radiopharmaceutical applications did not demonstrate plateauing at activity ranges explored for direct position detection [6] or Cherenkov radiation [7]. Overall, linearity with increasing activity is demonstrated and establishes the system's robustness and reinforces its capability to accurately monitor and quantify activity levels.

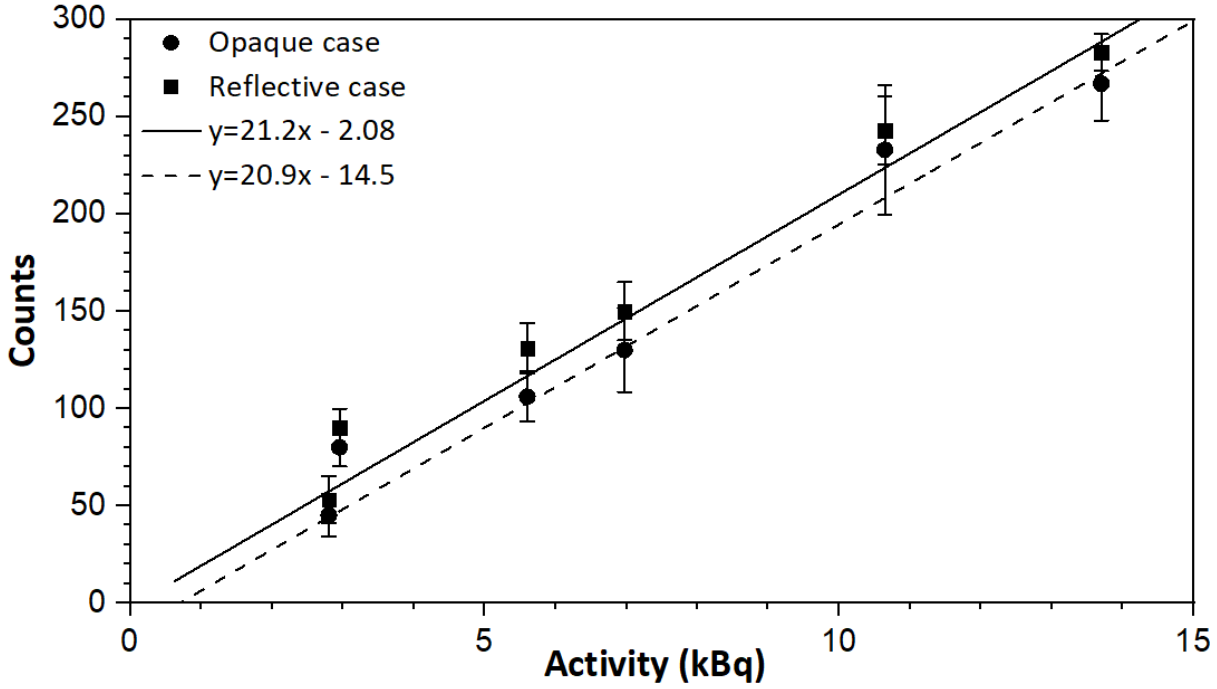

Figure 4. Comparison of PMT output in counts (over 5 minutes) opaque and reflective cases with increasing activity in prototype.

LIMIT OF DETECTION

The limit of detection (LoD) of a system describes the fewest number of counts which can be detected reliably by the system. This property is particularly relevant in the case developing monitoring technologies for radionuclide activity as it describes the lowest activity which can be detected. LoD in terms of counts is described by Equation 2[8].

$$LoD_{counts} = 2.71 + 4.65\sqrt{B} \quad \text{(Eq.2)}$$

Where B is the background. The average limit of detection was calculated across the average of five background measurements, each conducted over a 12-hour period with count times of 5 minutes and readings taken every 30 minutes. The limit of detection was determined to be 23 counts. In terms of minimum detectable activity which signifies the minimum activity level that can be reliably detected by each prototype scenario, as outlined Table 1. is described by Equation 3.

$$MDA = \frac{LoD_{counts}}{C_{time}} \cdot f \quad \text{(Eq.3)}$$

Where C_{time} is the count time and f is the radiation yield per disintegration. The minimum detectable activity was then corrected for the volume in the prototype. The MDA demonstrated that the reflective plane decreased the MDA slightly, and increased the sensitivity of the prototype, the presence of the reflective surface also decreased the detectable activity per litre.

Table 1. Minimum detectable activity for each MDU case.

Surface of Prototype	Minimum detectable activity / (kBq)	Activity (kBq/L)
Opaque	0.09	32.1
Reflective	0.08	28.6

To enhance the limits of detection and increase the sensitivity of the prototype, potential improvements can be made to MDA and LoD in future work. This could include extending the count times for background and active readings, extending the counting time, and increasing the number of readings, thereby reducing the statistical uncertainty associated with background radiation. Another avenue for improvement is the reduction of system noise and signal interference through filtering and deconvolution [9].

INTEGRATION WITH MODELLED SYSTEMS

Upon establishing the linear response of the prototype to activity, the next step was to compare the prototype with outcomes from analogous Finite Element Analysis (FEA) models. This comparison aimed to quantify and assess any parameters that could not be accurately modelled. The photon transport modelling was conducted using COMSOL Multiphysics® software with the Ray Tracing Optics module. The simulations involved followed boundary conditions and parameters from Lu et al., 2023 [1]. A Hamamatsu photomultiplier tube (PMT) detection window was used to represent the detector. The models incorporated refractive indices at a wavelength of 420 nm (peak of Cherenkov emission spectrum) for the materials involved. Water, with a refractive index of 1.33, represented the channel's media, and negligible absorption was assumed at 420 nm. The channel walls were configured with either an opaque surface (reflection coefficient of 0.04) or a reflective surface (reflection coefficient of 0.96). A perfect reflection coefficient of 1 was not applied in the reflective system to account for potential experimental setup defects. The detector's quantum efficiency was set at 1, and noise was directly modelled, as the detector's performance was not the primary focus.

The results were analysed by independently varying the activity and considering both reflective and opaque cases for each dimension change. The results revealed a good agreement ($R^2 > 0.91$) between the FEA model and the experimentally derived values (Figure 5). In both the reflective and opaque cases, the dual channel system exhibited a better agreement with the modelled results, with R^2 values exceeding 0.98 compared to the single channel system. This suggests that an increase in the number of photons that reach the detector improves the integration with modelled results.

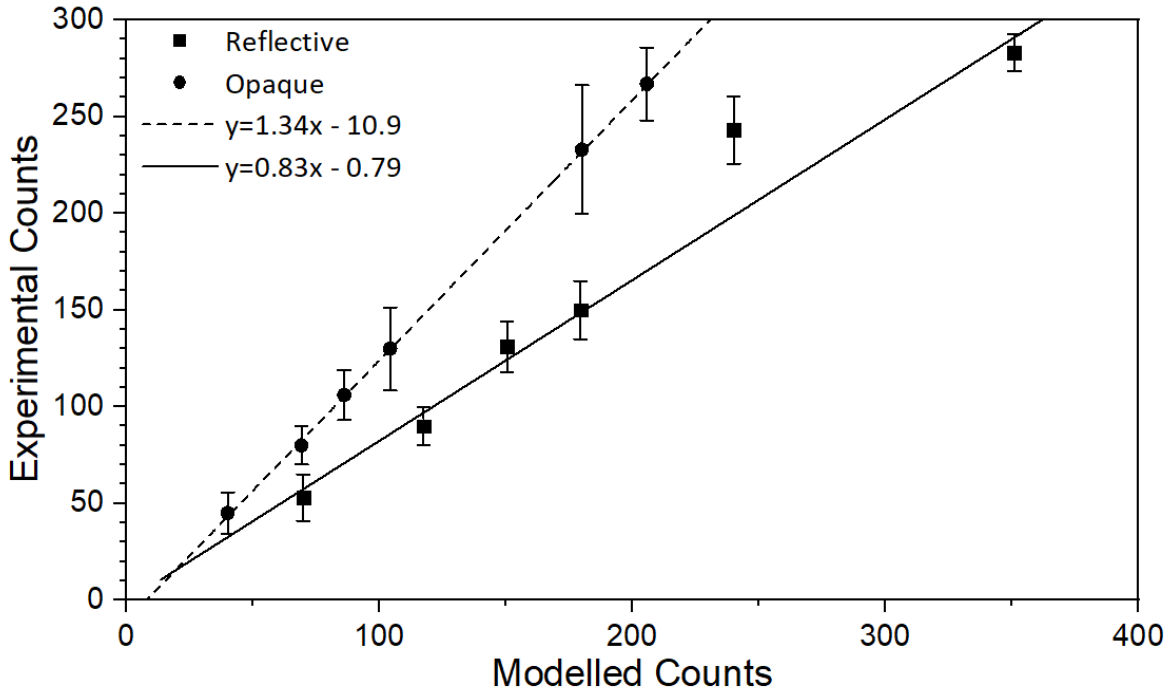

Figure 5. Comparison of modelled and experimental detector outputs of reflective and opaque cases. Linear regression has been applied to 6 points of the graph to demonstrate correlation between experimental and modelled results.

Results highlight that these numerical models can be used effectively to trend and optimise optical design features for radiometric microfluidic systems that rely on optical detection. This comparison between the prototypes and FEA models has provided valuable insights into their performance. The strong correlation observed validates the accuracy and reliability of the FEA models in predicting the behaviour of the prototypes. The results support the feasibility and effectiveness of the prototypes in detecting pure β-emitting radionuclides.

FLUSHING AND CARRYOVER

To evaluate the laboratory-based accuracy and precision of the prototype and provide insights for calibration improvements, a continuous flow experiment was conducted to measure sample carryover between samples. The experiment involved increasing activities to determine the time required for the first response and the time needed to return to the background level. The flow system consisted of a peristaltic pump (Watson Marlow 520 SR peristaltic pump, Watson & Marlow Ltd, UK) used to propel the ^{90}Sr solution (Figure 6). Teflon tubing (0.5 mm i.d. Merck, Germany) was used throughout the setup except for the peristaltic pump tubing (PVC Manifold 0.25 mm i.d. Watson & Marlow Ltd, UK). The setup was light occluded with a lid and blackout sheets to prevent stray photons from impacting the detector output.

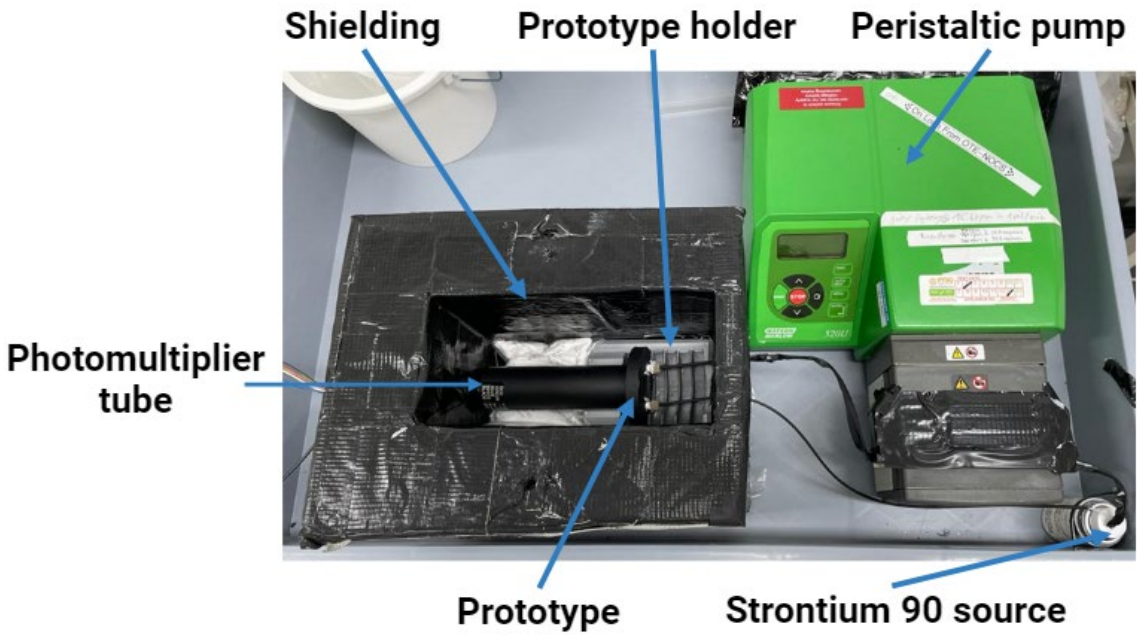

Figure 6. Picture of experimental setup for the sample carryover experiment, the setup is pictured without the blackout lid and sheets.

For the carryover and flushing experiments, the volume of the prototype, fill time, flow rate, sample residence time and emptying time of the full circuit were calculated experimentally to ensure reliable and consistent measurements (Table 2).

Table 2. Experimentally calculated fill time, flow rate, sample residence time and emptying time.

	Time /(min)
Prototype volume channel volume / (mL)	2.8
Fill time (full circuit) / (mins)	22
Flow rate (full circuit) / ($mLmin^{-1}$)	0.13
Sample residence time / (mins)	21.5
Emptying time (full circuit) / (mins)	27

For the flushing and carryover experiments a count time of 2 minutes was chosen to observe changes in the prototype system. The experimental results revealed a notable increase in sample carryover after reaching an activity level of 50 kBq, requiring approximately 22 minutes (Table 3) for the system to return to background levels compared to the mean time of 10 minutes for other activities. However, the system did not demonstrate any carry over that increased the baseline with increasing activity and the counts eventually returned to the baseline (Figure 7). In addition to this, the average background counts and standard deviation of these counts remained within a coefficient variation of <0.5 before and after sample spiking (Table 4). This finding emphasises the importance of evaluating the impact of the filling mechanism on the overall performance of the system to see if this impacts the time to first response or the time to return to background.

Table 3. Time to first response and return to background for each activity tested.

Activity (kBq)	Time to first response / (Minutes)	Time to return to background / (Minutes)
8	8	10
25	10	12
50	6	22
8	8	8

Table 4, Average background prior and post active sample introduction.

Activity (kBq)	Average	Standard deviation	Coefficient of variation
Before 8	9.86	3.85	0.39
After 8 /before 25	9.18	3.59	0.39
After 25 before 50	8.59	2.98	0.35
After 50	9.75	3.57	0.37
After 8	9.47	2.33	0.25

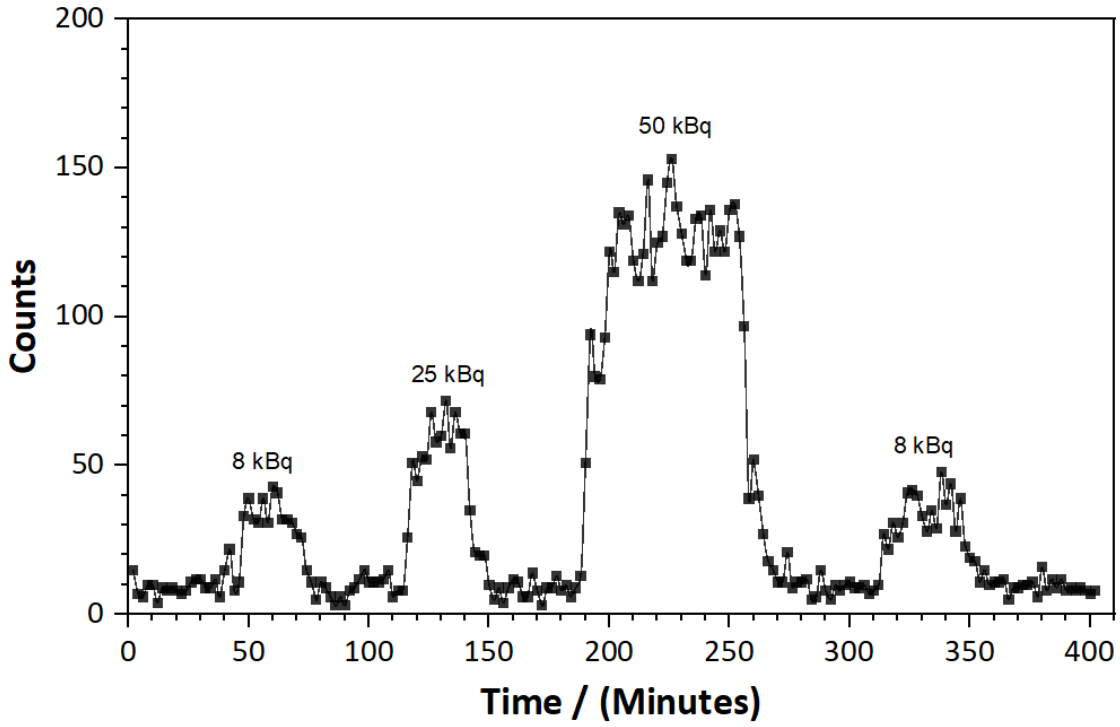

Figure 7. Continuous flow study of dual channel system, each data point represents a two-minute count.

These findings play a crucial role in optimising device deployment and minimising any potential impact on analysis results. To maintain data consistency over time, it is important to ensure that the baseline does not increase with each measurement of a high activity sample.

VALIDATION WITH ADDITIONAL RADIONUCLIDES

To comprehensively assess the efficiency of the prototype for different β emitters, three different radionuclides (^{99}Tc, ^{36}Cl and ^{90}Sr/Y) with β maximum energies (E_{max}) ranging between 298 – 2270 keV respectively loaded into the prototype separately. Counts were recorded at 5-minute intervals to capture the system's response to changing (E_{max}) levels. Count measurements were recorded every 30 minutes for a minimum of 3 hours. Due to the limitations of the counting system, the energy and number of β emissions for a given radionuclide cannot be differentiated between. Therefore, for this study, counts and uncertainties were activity corrected for each radionuclide (Table 5) to ensure count measurements only capture the system's response to changing (E_{max}) on photon production and therefore count rate. The same cleaning and loading procedures were followed as per linearity experiments. The results demonstrated linearity with an increasing energy range examined and the capability to measure different β emitting radionuclides. The logs of counts and uncertainties were taken and then plotted as a scaled count rate over 5 minutes to visualise linear relationship between E_{avg} and counts (Figure 8). The result from this work indicates that system could be further extended to low energy β emitters and α emitters through the incorporation of a solid or liquid scintillation system to examine lower activities and emission energies.

Table 5. Efficiency assessment of the prototype for different β emitters, with counts corrected to corresponding activity.

	Counts/ 5 minutes corrected for activity (kBq)		
	^{99}Tc (99 kEv)	^{36}Cl (236 kEv)	^{90}Sr/Y (760 kEv)
2.8 kBq	1.6	1.9	14
Uncertainty	1.1	1.2	1.2

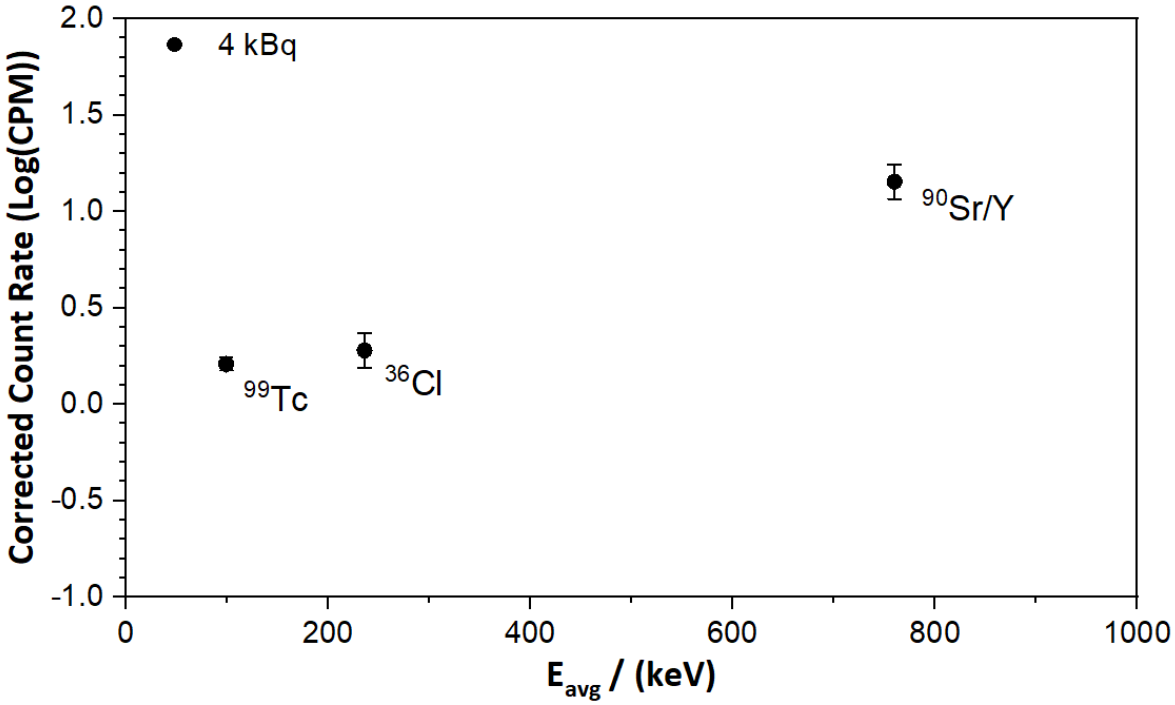

Figure 8. Efficiency assessment of the prototype for different β emitters, with log taken of corrected counts

CONCLUSION

This study advances Lab-on-a-Chip (LoC) systems for pure β-emitting radionuclide detection. A validated prototype has demonstrated feasibility for *in situ* detection of pure β emitters, with linear response to increasing activity. The prototype detected the presence of β particles through Cherenkov radiation, achieving a minimum detectable activity of 0.8 kBq. Numerical modeling and radiometric validation achieved R^2 >0.91 demonstrating the ability for this method to inform rapid prototyping and design improvements. Future work should target specific applications where the LoC device would be deployed and should explore integration with separation/pre-concentration systems for autonomous nuclide-specific detection. LoC systems have the potential to offer scalable, high-throughput, nuclide-specific measurements for advanced nuclear technologies. Simplified modeling parameters are vital for cost-effective prototyping. This technology holds potential for safer, more efficient nuclear industry practices by addressing sample handling, waste, and material cost challenges.

REFERENCES

[1] S.E. Lu, A. Morris, G. Clinton-Bailey, M. Namiq, P.C. Gow, A. Birchill, S. Steigenberger, J. Wyatt, R. Forrester, M.C. Mowlem, P.E. Warwick, Rapid prototyping Lab-on-Chip devices for the future: A numerical optimisation of bulk optical parameters in microfluidic systems, Sensors and Actuators A: Physical. 359 (2023) 114496. https://doi.org/10.1016/j.sna.2023.114496.

[2] K.J. Glennon, H.F. Valdovinos, T. Parsons-Davis, J.A. Shusterman, A.G. Servis, K.J. Moody, N. Gharibyan, 3D printed field-deployable microfluidic systems for the separation and assay of Pu in nuclear forensics, Lab Chip. 22 (2022) 4493–4500. https://doi.org/10.1039/D2LC00391K.

[3] C. Mariet, A. Vansteene, M. Losno, J. Pellé, J.-P. Jasmin, A. Bruchet, G. Hellé, Microfluidics devices applied to radionuclides separation in acidic media for the nuclear fuel cycle, Micro and Nano Engineering. 3 (2019) 7–14. https://doi.org/10.1016/j.mne.2019.02.006.

[4] G. Turkington, K.A.A. Gamage, J. Graham, Beta detection of strontium-90 and the potential for direct in situ beta detection for nuclear decommissioning applications, Nuclear Instruments and Methods in Physics Research Section A: Accelerators, Spectrometers, Detectors and Associated Equipment. 911 (2018) 55–65. https://doi.org/10.1016/J.NIMA.2018.09.101.

[5] I. Ogilvie, V. Sieben, C.F. Floquet, R. Zmijan, M. Mowlem, H. Morgan, Solvent processing of PMMA and COC chips for bonding devices with optical quality surfaces, 14th International Conference on Miniaturized System for Chemistry and Life Sciences. 1244–1246 (2010).

[6] M.P. Taggart, M.D. Tarn, M.M.N. Esfahani, D.M. Schofield, N.J. Brown, S.J. Archibald, T. Deakin, N. Pamme, L.F. Thompson, Development of radiodetection systems towards miniaturised quality control of PET and SPECT radiopharmaceuticals, Lab on a Chip. 16 (2016) 1605–1616. https://doi.org/10.1039/c6lc00099a.

[7] J.S. Cho, R. Taschereau, S. Olma, K. Liu, Y.C. Chen, C.K.F. Shen, R.M. Van Dam, A.F. Chatziioannou, Cerenkov radiation imaging as a method for quantitative measurements of beta particles in a microfluidic chip, Physics in Medicine and Biology. 54 (2009) 6757–6771. https://doi.org/10.1088/0031-9155/54/22/001.

[8] L.A. Currie, Limits for qualitative detection and quantitative determination. Application to radiochemistry, Anal. Chem. 40 (1968) 586–593. https://doi.org/10.1021/ac60259a007.

[9] R. Remetti, A. Sessa, Beta spectra deconvolution for liquid scintillation counting, J Radioanal Nucl Chem. 287 (2011) 107–111. https://doi.org/10.1007/s10967-010-0882-0.

ACKNOWLEDGMENTS

This work was supported by the Natural Environmental Research Council [grant number NE/N012070/1]